Chemokines in Ewing sarcoma

Sand, L.G.L.

Chapter 5

Novel splice variants of *CXCR4* identified by transcriptome sequencing

L.G.L Sand, A.G. Jochemsen, E. Beletkaia, T. Schmidt, P.C.W. Hogendoorn and K. Szuhai

Biochemical, Biophysical Research Communication, 2015, 466(1), 89-94

ABSTRACT

Chemokine receptor CXCR4 is involved in tumor growth, angiogenesis and metastasis. Its function is regulated in many ways and one of them is alternative splicing. We identified two novel coding splice variants (*CXCR4-3 and CXCR4-4*) of *CXCR4* in Ewing sarcoma (EWS) cell lines by whole transcriptome sequencing and validated these with reverse transcriptase- PCR and Sanger sequencing. The novel splice variants were expressed at RNA level in Ewing sarcoma samples and in other tumor cell lines and placenta, but not in lung. Due to inclusion of an additional exon the new isoforms have a 70 and 33 amino acid elongation of the N-terminal end of CXCR4. For validation at protein and functional level, the identified isoforms and normal CXCR4 were cloned into an EYFP tagged vector and ectopically expressed in HEK293T cell line and EWS cell line A673. Of the novel isoforms CXCR4-3 showed cell membrane localization and a functional response after addition of CXCR4 ligand CXCL12a. CXCR4-4 showed strong cytoplasmic accumulation and no response to ligand treatment. The role of the newly discovered isoforms in CXCR4 signaling is likely to be limited. Our data stresses the importance of functional validation of newly identified isoforms.

KEYWORDS

CXCR4; Splicing; Next generation sequencing; Ewing sarcoma; Bone tumors; Soft tissue tumor

INTRODUCTION

Chemokines are low molecular weight signaling proteins and characterized by a cysteine motif. The primary function of chemokines is related to inflammatory response and immune-surveillance. In addition, chemokines play a key role in tumor development and progression. The tumor microenvironment has a key role in growth, angiogenesis and metastasis [1-3]. Hence, chemokines show enhanced tumorigenic functions as they are involved in angiogenesis, tumor growth, immune suppression and metastasis[2]. The presence and activation of the chemokine receptor CXCR4 has been shown to be associated with metastasis and consequently decreased survival [4-6]. The function of CXCR4 is regulated at multiple levels both with regard to inter- and intracellular interactions through transcriptional processing via alternative splicing, posttranslational modifications and receptor dimerizations [7-10].

Ewing sarcoma (EWS), a highly malignant bone and soft tissue tumor, is characterized by a pathognomonic translocation between the *EWSR1* gene and a member of the ETS family of transcription factor genes [11-12]. The fusion protein influences, transcription, alternative splicing and protein–protein interactions [12]. The fusion protein is partly responsible for the aggressive growth, high vascularization and metastatic properties in EWS and in all these processes CXCR4 is involved. As the prognosis for EWS patients with established metastases at diagnosis or relapse remains dismal, investigation of the CXCR4 involvement in tumor progression and metastasis could be of clinical relevance [13-14]. RNA and protein studies have associated CXCR4 expression with various properties, like metastasis, tumor growth and survival [5,15]. Recently, we found that increased expression levels of CXCR7 and CXCL14, factors inhibiting CXCR4 signaling were associated with improved survival and, *vice versa*, the absence of these factors correlated with metastasis development [16]. Fur-

thermore, an improved survival was associated with the ratio between the known splice variants of CXCR4, *CXCR4-1* and *CXCR4-2*. These variants consist of either two exons dubbed as *CXCR4-2* or one exon by utilizing an alternative start codon inside intron one dubbed as *CXCR4-1* [22]. At the protein level, in the CXCR4-1 variant, compared to the CXCR4-2 variant, the first five amino acids at the N-terminus are replaced with nine other amino acids (**Figure 1**). As the N-terminus of CXCR4 is crucial in CXCL12 binding, the differences between the two splice variants may lead to an altered CXCR4 activation efficacy [10]. We performed transcriptome analysis using a next generation sequencing approach to identify new splice variants in Ewing sarcoma cell lines and tumor samples. Next to the earlier described splice variants of *CXCR4*, we identified two novel splice variants*CXCR4-3* and *CXCR4-4*, which resulted in a 70 and 33 amino acid extension of the receptor at the N-terminus domain, respectively. Although the novel isoforms were expressed, it is likely that function of these splice variants is limited. In addition, our work demonstrates that functional validation of novel isoforms identified by transcriptome analysis is necessary.

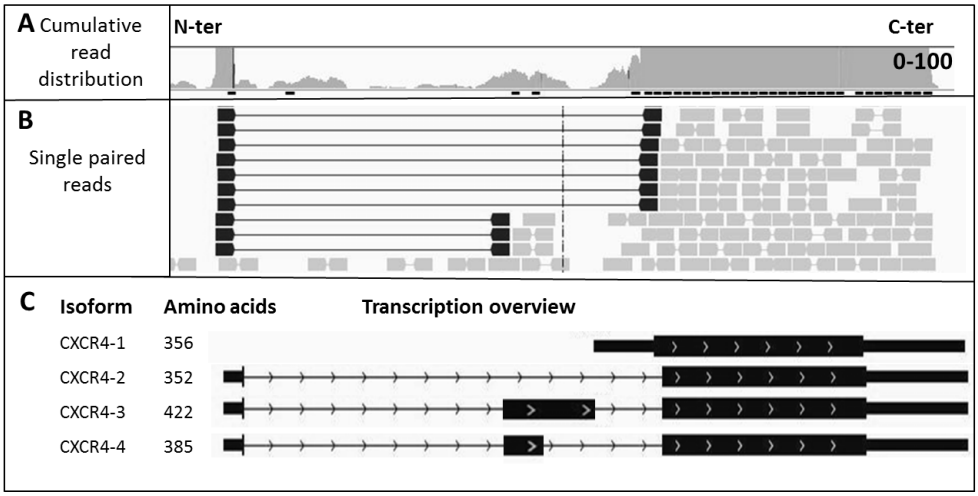

Figure 1: Identification of new CXCR4 isoforms. IGV plot of transcriptome sequencing data showing the potential alternative spliced exon in intron 1 of *CXCR4*. **A**) Read coverage of IGV plot at 0–100 read range and **B**) single alignments of whole transcriptome sequences of *CXCR4* from EWS cell line EW3 (black connected blocks are paired end reads over a large distance of the genome, marking exons). **C**) Overview of all*CXCR4* isoforms with the genomic position of the exons and number of amino acids when translated.

MATERIAL & METHODS

Ewing sarcoma cell lines

Twenty-three EWS cell lines and one primary culture were cultured as described by Sand *et al.* [16]. Human embryonic kidney cell line HEK293T was cultured in DMEM with 10% FCS without antibiotics; human T cell leukemia cell line Jurkat, colon carcinoma cell lines SW480, HT29 and HCT116; cervical carcinoma cell lines Hela, Siha and Caski; breast carcinoma cell lines MDA-MB-231 and MCF7 were obtained from ATCC[2] and cultured in RPMI with 10% heat inactivated FCS without antibiotics. All cell lines were regularly tested on mycoplasma and authentication with DNA Q-PCR screening and CellID STR, respectively (Promega, Leiden, The Netherlands).

Patient samples

Twenty-five frozen tumor samples from twenty EWS patients and two samples of lung and placenta were obtained from the Department of Pathology, Leiden University Medical Center. Eighteen tumor samples were therapy-naïve samples and seven were obtained post-chemotherapy samples, including three lung metastases and four local relapses. All tumor samples contained at least 80% tumor cells estimated by histological examination. All patient samples were handled in a coded fashion, according to the Dutch national ethical guidelines ('Code for Proper Secondary Use of Human Tissue').

RNA isolation

Total RNA was isolated from cell lines and tumor samples using TRIzol Reagent (Life Technologies). The RNA concentration and quality was established by using Nanodrop and Bioanalyzer2000 RNA Nano chip (Agilent Technology, Amstelveen, The Netherlands).

Whole transcriptome sequencing

RNA with a quality RIN value of eight of EWS cell lines EW3, CADO-ES1 and 6647 was sequenced by BGI genomics (Hong Kong, People's Republic of China) following their standard protocol as mentioned by Sand et al. [16]. Mapped reads were sorted and result files were visualized with Integrative Genomics Viewer (IGV) using UCSC Human genome built 19 as a reference [17-18].

Reverse transcriptase PCR, sequencing and reverse transcriptase-quantitative-PCR

For validation of transcriptome sequencing data, a sequencing primer pair was designed (**Table 1**). Amplified products generated with High Fidelity FAST-TAQ polymerase were analyzed by agarose gel (Life Technologies) and cloned into *pCR2.1* TOPO cloning vectors. Isolated plasmids were Sanger sequenced by Macrogen (Macrogen, Amsterdam, Netherlands) using *M13* tailed primers and sequences were aligned by blasting (NCBI). RNA expression of *CXCR4-3* and *CXCR4-4* together were obtained using in-house designed RT-Q-PCR primers (**Table 1**) and performed as described by Sand et al. [16].

Table 1: Primer sequences used for cloning and RT-Q-PCR

Name	Sequence
CXCR4seqF	5' GATCGGTACCATGGAGGGGATCAGTGAAAATG
CXCR4seqR	5' AAGGCCAGGATGAGGACACT
CXCR4rtpcrF	5' AGGTAGCAAAGTGACGCCGA
CXCR4rtpcrR	5' ATTTTCTGACACTCCCGCCC

CXCR4-3 and CXCR4-4 cloning, transfection and imaging

pCR2.1 TOPO cloning vectors containing *CXCR4-3* and *CXCR4-4* were cloned into a*pEYFP-N1* plasmid containing *CXCR4-2*. The resulting plasmids were quality controlled by BsteII-EcoRI digestion and sequencing using CMV-Fw and CXCR4-R primers.*pEYFP-N1 CXCR4-2*, *CXCR4-3* and *CXCR4-4* were transiently transfected into HEK239T and A673 cells using FuGENE HD (Promega, Leiden, The Netherlands). Imaging was performed next day in serum-free medium while kept at culture conditions using the INUBG2E-ZILCS (TokaiHit, Japan).

Calcium mobilization assay

Intracellular calcium level was determined using cell permeant Fluo4-AM (Life Technologies, The Netherlands). Cells were pre-incubated with 1 μM Fluo4-AM for 30 min. The Fluo4-AM fluorescence was detected using time-lapse confocal microscopy with a 488 nm excitation laser beam. After 30 s 100 nM of CXCL12a was added. Intensity change calculations were done using in-house developed scripts in MatLab (Mathworks Inc., Massachusetts, USA).

Western blot

Transfected HEK293T and A673 cells were lysed 48 h after transfection and were treated 6 h before lysis with 10 μM MG132 proteasome inhibitor (Sigma–Aldrich). Cell lysates were prepared using Giordano buffer (50 mM Tris–HCl, pH 7.4, 0.1% Triton X-100, 250 mM NaCl, 5 mM EDTA) containing phosphatase and protease inhibitors (Sigma–Aldrich). After blotting and blocking with 10% low fat skimmed milk, membranes were stained with anti-GFP (Rabbit, 1:1000,GeneTex, Alton, US).

In silico prediction software

Splice sites were predicted by ASSP software using as input complete sequence of CXCR4 gene according to UCSC hg19 genome reference, using the standard settings [19]. With this software tool, predicted splice sites considered to be positive above threshold value of four and above seven the false positive discovery rate considered to be minimal.

RESULTS

Identification of splice variant of *CXCR4*

mRNA from EW3, CADO-ES and 6647 EWS cell lines were analyzed by transcriptome sequencing using deep sequencing approach with paired-end reads. Sequence read files were mapped to coding regions of the genome and visualized with IGV application (**Figure 1A,B**). A tiling coverage of paired-end reads in intron 1 were observed. These read pairs were connected to exon 1 and to exon 2 of CXCR4, indicating the presence of additional transcribed splice variants (**Figure 1B**).

Putative splice sites were *in silico* searched in the entire *CXCR4* DNA sequence. At the 5' end of the newly identified exon one splice donor site and multiple acceptor splice sites were predicted (**Table 2**). The probability scores varied between 5 and 9, out of the maximal score of 16 indicating a strong likelihood of true splice sites. For experimental verification a sequencing primer pair covering the complete new exon, including an exon 1 and new exon overlapping forward primer were designed (**Table 1**). Amplification of the putative exon resulted in a PCR product with two different lengths after gel electrophoresis size separation. The amplified products were cloned and sequenced using Sanger sequencing. With the sequencing we identified two novel splice variants as a result of splicing of a novel exon in the *CXCR4* gene. Splicing-in at the predicted splice acceptor site and the splice donor sites #3 and #2 resulted in two in-frame splice variants *CXCR4-3* with an addition of 210 bp of the new exon and *CXCR4-4*with an addition 99 bp of the new exon (**Figure 1C**). Translation of these new isoforms resulted in elongation of N-terminus of CXR4 with 70 (CXCR4-3) or 33 (CXCR4-4) amino acids compared to CXCR4-2.

Table 2: Predicted splice sites in the CXCR4 intron

Position	Sequence	Score[a]
Splice site donor		
potential Start new exon	ctccaccag**GAAAATGCCC**	8.9
Splice site acceptor		
potential End new Exon#1	**AACGCGCCAA**gtgataaaca	4.9
potential End new Exon#2	**GGGGGAGGAG**gtgccgtttg	6.3
potential End new Exon#3	**GCCCAGAATG**gtttgtattt	7.6

[a] Composed score reflecting strength of splice site by using ASSP tool, a threshold of 4 was used to limit false positive [19]. Capital letter represent coding sequence

Analysis of new CRCR4 isoform expression in clinical samples

RNA expression of the separate new splice variants could not be obtained since exon overlapping RT-Q-PCR primers could not be designed, while primers for obtaining expression of both splice variants could be established (**Table 1**). RNA expression was analyzed in Ewing sarcoma cell lines and tumor samples, in a panel of cancer cell lines and HEK293T cell line together with normal lung and placenta tissues. In fourteen of the twenty five EWS samples expression was detected, consisting of eleven primary therapy-naïve tumors and three metastatic or recurrent tumor samples. Sixteen of the twenty-three EWS cell lines showed expression of the new splice variants (**Table 3**). Of the analyzed normal tissues samples only placenta, but not lung tissue showed expression (**Figure 2A**). When the expression of *CXCR4-2* was used as a reference, the measured expression was found to be much higher than the novel variant (**Figure 2B**).

Table 3: Expression of CXCR4-3 and CXCR4-4 together in Ewing sarcoma tumor samples and cell lines (% of total)

	EWS tumor samples		EWS cell lines/primary cultures
	Primary	Metastasis/relapse	
RNA expression	11/18 (61%)	3/7 (43%)	16/23 (70%)

Protein analysis and cellular distribution of novel CXCR4 isoforms

The expression and cellular distribution of the novel CXCR4 protein isoforms, CXCR4-3 and CXCR4-4, were studied using pEYFP-N1 tagged plasmid vectors in the HEK293T cell line and A673 EWS cell lines. As control the CXCR4-2-pEYFP-N1 plasmid transfection was used. The ectopically expressed CXCR4-2 protein was localized at the cell membrane, while

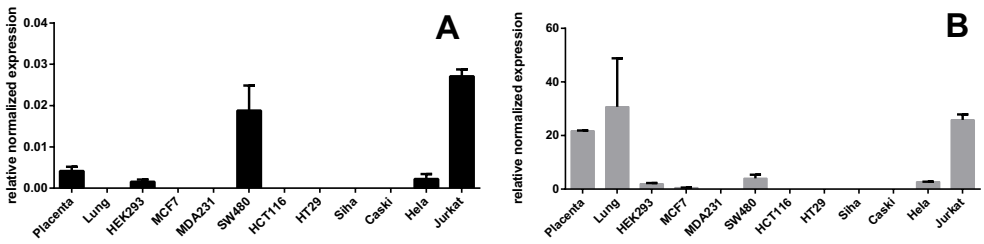

Figure 2: Expression of the novel splice variants in cell line and tissue panel. Housekeeping gene normalized expression of (**A**) new CXCR4 exon and of (**B**) *CXCR4-2* in tissue and cell lines (mean ± SEM, n = 3). The highest expression of the novel splice variants was detected in Jurkat and SW480 cell lines.

CXCR4-4 showed a sole cytoplasmic distribution. For CXCR4-3 differences were observed between A673 and HEK293T, with only a cytoplasmic localization detected in A673 and both a membrane and cytoplasmic localization detected in HEK293T (**Figure 3A**). To further compare the expression levels and molecular weight of the different isoforms all three isoforms were analyzed by western blot using anti-GFP antibody (**Figure 3B**). Despite using an identical vector construct in HEK293T cell line, the expression levels of CXCR4-3 and CXCR4-4 were remarkably lower compared to the expression level of CXCR4-2. Intriguingly, the expression of CXCR4-3 and CXCR4-4 protein isoforms was below the detection limit in A673 cell line. Transfected cell lines were then treated with MG132 proteasome inhibitor that resulted in an increased expression of the CXCR4-3 and CXCR4-4 in both cell lines indicating that the isoforms were unstable and the majority of expressed protein was degraded. The calculated molecular weights without any possible post-translational modification for CXCR4-2, CXCR4-3 and CXCR4-4, including the YFP tag, are 66.6, 70.3 and 74.6 kDa, respectively. Western blot analysis showed multiple bands with two dominant ones at ~65 and 70 kDa of the CXCR4-2 protein (**Figure 3B**). When comparing the lanes from CXCR4-3 and CXCR4-4 we observed that CXCR4-3 has an increased molecular weight, corresponding to the calculated molecular weight. However, for CXCR4-4 transfected samples, bands lower than the calculated molecular weight with size comparable to CXCR4-2 were observed indicating the possibility of protein cleavage for this splice variant. As even after proteasome inhibitor treat-

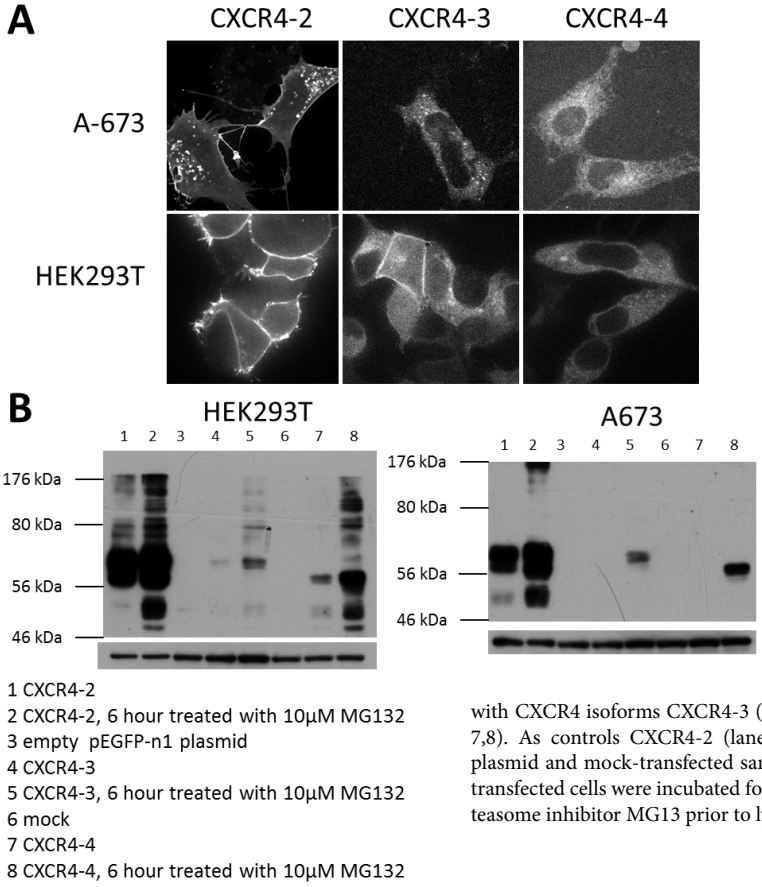

Figure 3: CXCR4 isoforms subcellular localization and protein expression. A) Representative images from transient transfection experiment with the three different CXCR4 isoforms expressed in A673 and HEK293T cell line. Life cells were imaged with a spinning-disc confocal microscope. CXCR4-2 was dominantly localized at the cell membrane in both cell lines. CXCR4-3 showed cytoplasmic localization in A673 cells and partial membrane localization in HEK293T cells. CXCR4-4 exhibited only cytoplasmic localization in both cell lines. **B**) Western blots of transiently transfected HEK293T and A673 cells with CXCR4 isoforms CXCR4-3 (lane 4,5), CXCR4-4 (lane 7,8). As controls CXCR4-2 (lane 1,2), empty pEYFP-N1 plasmid and mock-transfected samples were used. Isoform transfected cells were incubated for 6 h with or without proteasome inhibitor MG13 prior to lysis.

ment the expression levels of CXCR-3 and CXCR-4 were relatively low the RNA expression levels of the *CXCR4-EYFP* isoforms were analyzed. For this we designed primers annealing on *CXCR4* and *EYFP* parts, to amplify transfected CXCR4 variant only and a primer pair that *neo* selection gene expression that was present in the transfection vector to analyze relative transfection efficiency **(Figure 4A,B**). Transfection efficiency was estimated by comparing *CXCR4-3* and *CXCR4-4* expression levels to *CXCR4-2* and were found to be 3 and 10 fold lower, respectively (**Figure 4C**).

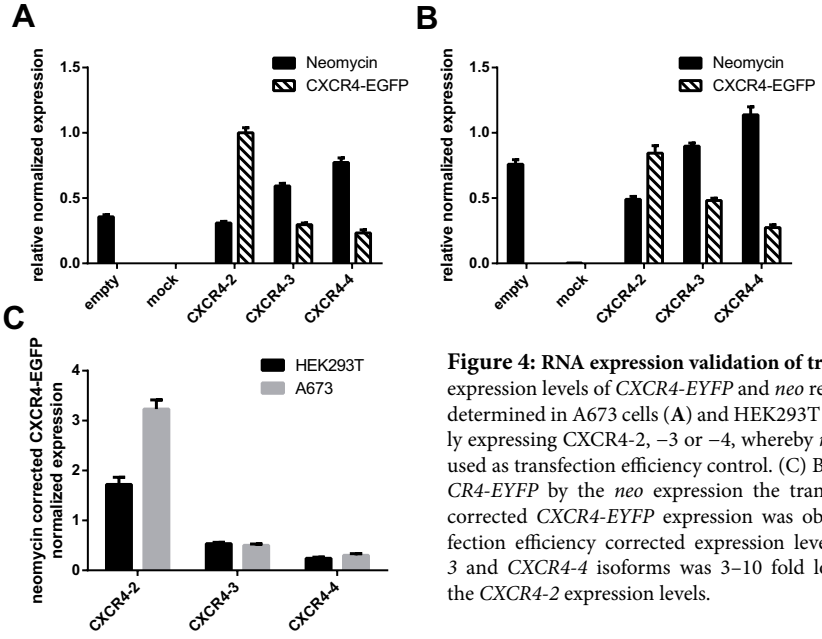

Figure 4: RNA expression validation of transfections. RNA expression levels of *CXCR4-EYFP* and *neo* resistance gene were determined in A673 cells (**A**) and HEK293T cells (**B**) ectopically expressing CXCR4-2, −3 or −4, whereby *neo* expression was used as transfection efficiency control. (C) By dividing the *CXCR4-EYFP* by the *neo* expression the transfection efficiency corrected *CXCR4-EYFP* expression was obtained. The transfection efficiency corrected expression levels of the *CXCR4-3* and *CXCR4-4* isoforms was 3–10 fold lower compared to the *CXCR4-2* expression levels.

Calcium mobilization assay

The activity of the receptor isoforms after CXCL12 stimulation was determined by a Ca^{2+}mobilization assay [20]. Upon binding of CXCL12 to CXCR4 receptor a downstream signaling gets activated that include calcium ions influx response. In A673 and HEK293T cells transfected with *CXCR4-2*, *CXCR4-3* or *CXCR4-4* plasmid the Ca^{2+} influx was measured over time before and after CXCL12a administration (**Figure 5**). For A673, only the *CXCR4-2* transfected cells demonstrated a clear effect. All HEK293T cells, including non-transfected cells, demonstrated an effect, indicating activation of some of the endogenous CXCR4 receptors. However, HEK293T cells transfected with *CXCR4-2* or*CXCR4-3* exhibited an elevated Ca^{2+} influx compared to non-transfected cells, suggesting that these receptors were activated by CXCL12a.

DISCUSSION

Two splice variants of CXCR4 have been identified earlier, *CXCR4-1* consisting of one exon only and the most dominantly expressed *CXCR4-2* existing of two exons. Using whole transcriptome analysis in EWS cell lines we discovered two novel CXCR4 splice variants *CXCR4-3* and *CXCR4-4*. The new splice variants were expressed in EWS tumor and cell line samples

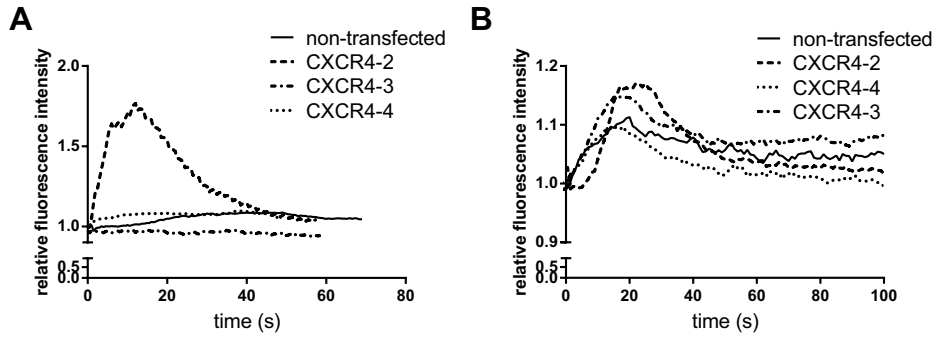

Figure 4: CXCR4 isoform activity indirectly measured by calcium influx. Cell lines A673 (**A**) and HEK293T (**B**) transfected with CXCR4-2, CXCR4-3 or CXCR4-4 constructs were pre-incubated with Fluo4-AM for 30 min. Time-lapse life cell confocal imaging prior to and after administration of 100 nM CXCL12a was performed. A representative graph of the relative fluorescence intensity change of Fluo4-AM over time is shown (n = 3).

and other tumor cell lines and in placenta indicating that its expression is not a Ewing sarcoma specific event. The expression of both splice variants together was more than ten-fold lower than expression of the canonical *CXCR4-2* isoform. Notably, none of the samples showed expression of the splice variants without the expression of *CXCR4-2*. This implies that the expression of the new isoforms is depended on the upstream promoter used for *CXCR4-2*. With the use transcriptome sequencing the number of novel splice variants detected has increased largely. A substantial part of these variants are coding. However, the function of these novel isoforms mostly is unknown. The identified novel CXCR4 isoforms were mainly localized in the cytoplasm and largely degraded by the proteasome. Similarly, a difference in protein stability in cells has been observed for two protein isoforms encoded by the *HDMX* gene. The HDMX-S isoform was reported to be more potent p53 inhibitor than HDMX and its mRNA was detected to be expressed in various tumors. However, functional test showed that this protein was unstable [21-23]. These results stress the importance to examine novel identified RNA splice variants for functionality at the protein level.

CXCL12 is the main ligand to activate CXCR4. The importance of the CXCR4 N-terminus in CXCL12 binding has been demonstrated by various models [24-28]. Changes in the N-terminus, like the CXCR4-1 isoform led to reduced CXCL12 affinity [10]. Interestingly, all reported CXCR4 isoforms, including the novel isoforms reported here, vary only at the N-terminus, suggesting that splicing might be a method to regulate CXCR4 ligand binding [10]. Our functional activity test of the novel CXCR4 isoforms revealed a minor increase in Ca^{2+} influx in *CXCR4-3* transfected HEK293T cells upon CXCL12a stimulation, implying functionality of CXCR4-3 (**Figure 5**).

Western blot analysis of CXCR4 protein with various antibodies regularly results in multiple bands as reported in the literature, for which post-translational protein modifications are thought to be the main reason [9, 29-30]. In HEK293T lysates multiple bands were observed for the ectopically expressed CXCR4 isoforms (**Figure 3B**). In A673 less bands were observed, implying variations in post-translational modifications of CXCR4, which has been reported in other cell lines [9]. Directed mutagenesis of post-translation modification sites in CXCR4-2 influenced the cellular localization of CXCR4-2 [30]. Lack of these modifications might explain the lack of additional bands in observed in CXCR4-3 transfected A673 cells and might be connected to the lack of membrane localization (**Figure 3A**). For CXCR4-4, the detected band in both cell lines exhibited lower molecular weight (~65 kDa) than expected

(≥70.3 kDa) (**Figure 3B**). This could be the result of a splice site introduced during cloning or cleavage of the protein. We tested the first possibility by PCR but no splice site was introduced. The presence of a C-terminal protein cleavage is unlikely as the detection was done by using an EYFP antibody and EYFP is localized at C-terminal end. We could not prove the N-terminal cleavage of CXCR4-4. However, N-terminal cleavage has been reported for ectopically expressed CXCR4-2 variant that led to reduced membranous expression [29-30]. Thus, N-terminal cleavage might also explain the cytoplasmic localization observed for CXCR4-4 in HEK293T and A673 cells.

In conclusion, we have identified and validated novel *CXCR4* isoforms *CXCR4-3* and*CXCR4-4*, which contained a novel spliced-in exon, leading to a N-terminal protein elongation of 70 and 33 amino acids, respectively. These novel isoforms are low expressed compared to the dominantly expressed canonical *CXCR4-2* isoform in all cells tested and are expressed in cell lines, tumor samples and placenta. Ectopically expressed CXCR4-3 and CXCR4-4 proteins appear to be unstable, possibly caused by the unfolded-protein response. Localization slightly varied between the tested cell lines. Cell membrane and cytoplasmic localization of the CXCR4-3 protein was observed only in HEK293T cells. Functionality of the ectopically expressed receptors was tested upon CXCL12a stimulation and we observed in both CXCR4-2 transfected cell lines receptor activation. Out of the two novel isoforms only CXCR4-3 was functional. Taken together the data, we show that CXCR4-3 isoform, despite the observed instability and partial cell membrane localization, is functional upon CXCL12a stimulation, while any activity of CXCR4-4 is absent. In addition, our data shows the importance of functional validation of novel identified isoforms.

ACKNOWLEDGMENTS

This study was supported by National organization for Scientific Research (NWO) Grant-NWO-TOP GO 854.10.012 and we thank Inge Briaire-de Bruijn for technical support and Stefano Marullo for supplying the *CXCR4-2 pEYFP-N1* plasmid.

REFERENCES

1 Whiteside, T. L. The tumor microenvironment and its role in promoting tumor growth. *Oncogene* **27**, 5904-12, (2008).
2 Roussos, E. T., Condeelis, J. S. & Patsialou, A. Chemotaxis in cancer. *Nat Rev Cancer* **11**, 573-87, (2011).
3 Quail, D. F. & Joyce, J. A. Microenvironmental regulation of tumor progression and metastasis. *Nat Med* **19**, 1423-37, (2013).
4 Lippitz, B. E. Cytokine patterns in patients with cancer: a systematic review. *Lancet Oncol* **14**, e218-e28, (2013).
5 Berghuis, D. *et al.* The CXCR4-CXCL12 axis in Ewing sarcoma: promotion of tumor growth rather than metastatic disease. *Clin Sarc Res* **2**, 24, (2012).
6 Kim, J. *et al.* Chemokine Receptor CXCR4 Expression in Colorectal Cancer Patients Increases the Risk for Recurrence and for Poor Survival. *J Clin Oncol* **23**, 2744-53, (2005).
7 Ziarek, J. J. *et al.* Sulfopeptide Probes of the CXCR4/CXCL12 Interface Reveal Oligomer-Specific Contacts and Chemokine Allostery. *ACS Chem Biol* **8**, 1955-63, (2013).
8 Zhu, L., Zhao, Q. & Wu, B. Structure-based studies of chemokine receptors. *Curr Opin Struct Biol* **23**, 539-46, (2013).
9 Sloane, A. J. *et al.* Marked structural and functional heterogeneity in CXCR4: Separation of HIV-1 and SDF-1[alpha] responses. *Immunol Cell Biol* **83**, 129-43, (2005).
10 Gupta, S. K. & Pillarisetti, K. Cutting Edge: CXCR4-Lo: Molecular Cloning and Functional Expression of a Novel Human CXCR4 Splice Variant. *J Immunol* **163**, 2368-72, (1999).
11 De Alava, E., Lessnick, S. L. & Sorensen, P. H. in *WHO Classification of Tumors of Soft Tissue and Bone*

(eds C.D.M. Fletcher, J.A. Bridge, P. C. W. Hogendoorn, & F. Mertens) 306-9 (IARC, 2013).
12 Sand, L. G. L., Szuhai, K. & Hogendoorn, P. C. W. Sequencing overview of Ewing sarcoma: a journey across genomic, epigenomic and transcriptomic landscapes. *Int J Mol Sci* **16**, 16176-215, (2015).
13 Balamuth, N. J. & Womer, R. B. Ewing's sarcoma. *Lancet Oncol* **11**, 184-92, (2010).
14 Ladenstein, R. *et al.* Primary disseminated multifocal Ewing sarcoma: results of the Euro-EWING 99 trial. *J Clin Oncol* **28**, 3284-91, (2010).
15 Bennani-Baiti, I. M. *et al.* Intercohort Gene Expression Co-Analysis Reveals Chemokine Receptors as Prognostic Indicators in Ewing's sarcoma. *Clin Cancer Res* **16**, 3769-78, (2010).
16 Sand, L. G. L. *et al.* CXCL14, CXCR7 expression and CXCR4 splice variant ratio associate with survival and metastases in Ewing sarcoma patients *Eur J Cancer*, (2015).
17 Thorvaldsdóttir, H., Robinson, J. T. & Mesirov, J. P. Integrative Genomics Viewer (IGV): high-performance genomics data visualization and exploration. *Briefings in Bioinformatics* **14**, 178-92, (2013).
18 Robinson, J. T. *et al.* Integrative genomics viewer. *Nat Biotech* **29**, 24-6, (2011).
19 Wang, M. & Marín, A. Characterization and prediction of alternative splice sites. *Gene* **366**, 219-27, (2006).
20 Princen, K., Hatse, S., Vermeire, K., De Clercq, E. & Schols, D. Evaluation of SDF-1/CXCR4-induced Ca2+ signaling by fluorometric imaging plate reader (FLIPR) and flow cytometry. *Cytometry Part A* **51A**, 35-45, (2003).
21 Rallapalli, R., Strachan, G., Cho, B., Mercer, W. E. & Hall, D. J. A Novel MDMX Transcript Expressed in a Variety of Transformed Cell Lines Encodes a Truncated Protein with Potent p53 Repressive Activity. *J Biol Chem* **274**, 8299-308, (1999).
22 Lenos, K. *et al.* Alternate Splicing of the p53 Inhibitor HDMX Offers a Superior Prognostic Biomarker than p53 Mutation in Human Cancer. *Cancer Res* **72**, 4074-84, (2012).
23 de Lange, J. *et al.* High levels of Hdmx promote cell growth in a subset of uveal melanomas. *Am J Cancer Res* **2**, 492-507, (2012).
24 Brelot, A., Heveker, N., Montes, M. & Alizon, M. Identification of Residues of CXCR4 Critical for Human Immunodeficiency Virus Coreceptor and Chemokine Receptor Activities. *J Biol Chem* **275**, 23736-44, (2000).
25 Zhou, N. *et al.* Structural and Functional Characterization of Human CXCR4 as a Chemokine Receptor and HIV-1 Co-receptor by Mutagenesis and Molecular Modeling Studies. *J Biol Chem* **276**, 42826-33, (2001).
26 Xu, L., Li, Y., Sun, H., Li, D. & Hou, T. Structural basis of the interactions between CXCR4 and CXCL12/SDF-1 revealed by theoretical approaches. *Mol Biosyst* **9**, 2107-17, (2013).
27 Tamamis, P. & Floudas, C. A. Elucidating a Key Component of Cancer Metastasis: CXCL12 (SDF-1α) Binding to CXCR4. *J Chem Inf Model* **54**, 1174-88, (2014).
28 Qin, L. *et al.* Crystal structure of the chemokine receptor CXCR4 in complex with a viral chemokine. *Science* **347**, 1117-22, (2015).
29 Chabot, D. J., Chen, H., Dimitrov, D. S. & Broder, C. C. N-Linked Glycosylation of CXCR4 Masks Coreceptor Function for CCR5-Dependent Human Immunodeficiency Virus Type 1 Isolates. *J Virol* **74**, 4404-13, (2000).
30 Wang, J. *et al.* N-linked glycosylation in the CXCR4 N-terminus inhibits binding to HIV-1 envelope glycoproteins. *Virology* **324**, 140-50, (2004).